Sanchez *et al. Fire Ecology* (2026) 22:12
https://doi.org/10.1186/s42408-025-00442-8

Fire Ecology

RESEARCH

Open Access

Severity and recovery of post-fire vegetation cover using satellite images and burned area indices in Cajamarca (Peru)

Jefferson A. Cubas Sanchez[1,2], Candy Lisbeth-Ocaña Zúñiga[3*], Heinz Gonzáles Pérez[1], Almites Santos Moreno[4], Mario Ruiz Ramos[1], Elgar Barboza[5] and Alex J. Vergara[6]

Abstract

Background Assessing the severity of forest fires allows us to identify changes that compromise the natural regeneration capacity of vegetation. In this study, we evaluated the severity and recovery of vegetation after a fire using Sentinel-2 satellite images for the Cajamarca department in northeastern Peru. Hot spots were downloaded from the Fire Information for Resource Management System (FIRMS). This allowed us to identify eight groups with an area > 100 hectares, heat intensity > 100 Fire Radiative Power (FRP), and the presence of trees. By applying the Normalized Burn Ratio (NBR) and the Normalized Difference Vegetation Index (NDVI), the levels of extreme, high, medium, and low severity were determined, as well as the recovery of vegetation before and after the fire events.

Results and Conclusions The results indicated that 71.02% of the evaluated territory had low severity, 21.95% had medium severity, 6.41% had high severity, and 0.65% had extreme severity, indicating a prevalence of medium to low severity in the study area. The fires that occurred had similar NDVI levels in the pre-fire stage; however, after the fire, a progressive recovery of vegetation was observed in the study area. This highlights the application of spectral indices to assess the impact and regrowth of vegetation after the development of fires.

Keywords Forest fire management, Forest degradation, Spectral indices, DNBR, Google Earth Engine

Resumen

Antecedentes Determinar la severidad de incendios forestales nos permite identificar cambios que comprometen la capacidad natural de regeneración de la vegetación. En este estudio, evaluamos la severidad y recuperación de la vegetación luego de un incendio, usando imágenes del satélite Sentinel-2 para el departamento de Cajamarca en el noreste del Perú. Los puntos calientes fueron bajados del sistema de información sobre incendios para el manejo de Recursos (FIRMS en idioma Inglés). Esto nos permitió identificar ocho grupos con un área >100 ha, intensidad del fuego >100 usando el poder de radiación del fuego (FRP), y la presencia de árboles. Mediante la aplicación de la relación del Índice que Quemas Normalizado (NBR) y el índice de vegetación de diferencia normalizada (NDVI), los niveles de severidad extrema, media, y baja fueron determinados como así también la recuperación de la vegetación antes y después de eventos de fuego.

*Correspondence:
Candy Lisbeth-Ocaña Zúñiga
candy.ocana@unj.edu.pe
Full list of author information is available at the end of the article

Resultados y Conclusiones Los resultados indicaron que el 71,02 % del territorio evaluado tuvo una baja severidad, 21,95 % tuvo una severidad media, un 6,41% una severidad alta, y un 0,65% una severidad extrema del fuego, indicando la prevalencia de severidades medias a bajas en el área de estudios. Los fuegos ocurridos tuvieron similares niveles de NDVI en el pre-fuego. Sin embargo, luego del fuego, una recuperación progresiva de la vegetación fue observada en el área de estudios. Esto subraya la utilidad de la aplicación de índices espectrales para determinar el impacto y recrecimiento de la vegetación luego del desarrollo de incendios.

Introduction

Wildfires can pose a serious threat to the natural environment and public safety (Jaafari et al. 2018; Zhang et al. 2018). These events occur due to the existence of a fire source that can be originated both naturally and by human actions (Dentoni & Muñoz 2012; Kolanek et al. 2021; Marques et al. 2021). Forest fires are considered the main source of ecological degradation (Sudhakar et al. 2020) and modify the dynamics of natural ecosystems (Tonbul et al. 2016). They are currently the subject of intense research worldwide to develop prevention and mitigation strategies (Gonçalves et al. 2024).

Different factors such as vegetation characteristics, climatic conditions, and terrain topography can favor the spread of fire in different parts of the world (Dentoni & Muñoz 2012; Singh et al. 2022). Fires are mainly related to the development of anthropogenic activities, such as agriculture, livestock, and urban growth (Comisión Nacional Forestal [CONAFOR], 2010; Kolanek et al. 2021; Mabaso et al. 2022). According to Caraveo (2013), fires are one of the main hazards for forests and the environment, given that they increase greenhouse gas emissions and affect ecosystems showing different levels of severity (Botella & Fernández 2017; Liu et al. 2021).

According to García-Llamas et al. (2020), fire severity is an important variable for the prediction of post-fire vegetation recovery and succession, as it integrates the active characteristics of the fire and the immediate effects on the local environment (Shvetsov et al. 2019). Severity level is a descriptive concept that encompasses the physical, chemical, and biological alterations experienced by an ecosystem as a consequence of fire (McLauchlan et al. 2020; Smith et al. 2018; White et al. 1996). Likewise, high severity is related to low vegetation resilience and to factors that contribute to its deterioration and changes in its natural state (Flores et al. 2021). In general, fire severity is directly related to vegetation regeneration processes: the more intense the fire, the longer the recovery period (Caraveo 2013).

Vegetation recovery processes after a fire can vary significantly according to place and time, which makes it difficult to identify patterns or models (Gonzáles et al. 2024; Naveh 1990). Plant regeneration capacity is one of the most relevant indicators to evaluate the recovery of ecosystems affected by fire and is strongly influenced by soil characteristics and the type of climate present in the area. Despite their negative consequences, forest fires play essential roles in many forest processes; for example, they influence the composition and stages of succession and act as a selective factor for plant traits (Mohajane et al. 2021). Therefore, understanding post-fire forest recovery is fundamental to the study of forest dynamics and global carbon cycling (Meng et al. 2018).

Traditional techniques for monitoring forest fires are expensive and time-consuming, and their application in large remote forested areas is of little benefit (Kurbanov et al. 2022). In view of this, several researchers have employed remote sensing to assess vegetation regrowth and monitor fire severity (Pérez-Cabello et al. 2021; Storey et al. 2016; Vo & Kinoshita 2020). This technique obtains spectral information that allows to clearly differentiate areas affected by fire from those with vegetation cover (Chuvieco 2001). In addition, the combination of remote sensing with geographic information systems (GIS) has been key to understand the behavior of vegetation and its recovery after fire (Caraveo 2013). Similarly, remote sensing techniques have facilitated the study of vegetation regeneration processes from spectral information (Díaz-Delgado & Pons 2001).

Recent studies have employed artificial neural networks and machine learning as modeling approaches to achieve high accuracy in wildfire analysis (Piao et al. 2022). According to Sidhu et al. (2018), computing platforms facilitate open access to large datasets and increase the possibilities for analysis, including the availability of satellite imagery in large volumes. In this context, Google Earth Engine (GEE) has established itself in recent years as a key platform offering advanced services to the scientific community (Piao et al. 2022). GEE is a cloud-based satellite image processing tool, which stands out for its high computational speed and its ability to be applied to large areas (Piao et al. 2022; Singh et al. 2022). It also enables efficient assessment of fire status (Singh et al. 2022) and allows semi-automated and systematic monitoring of spectral severity indices (Parks et al. 2018; Silva-Cardoza et al. 2021). The assessment of vegetation severity and recovery by remote sensing provides essential mapping

information for post-fire action planning, such as reforestation, monitoring of vegetation regeneration, or soil protection against possible erosion processes (Caraveo 2013). Worldwide, several studies have used remote sensing techniques to evaluate regeneration and severity of forest fires (Morante-Carballo et al. 2022; Morresi et al. 2019; Pérez-Cabello et al. 2021; Shvetsov et al. 2019; Vo & Kinoshita 2020); however, in Peru, work in this field is still limited.

The estimation of forest fire risks is uncertain due to factors such as the presence of compound events, the interaction between fire and vegetation, and social aspects (Gonçalves et al. 2024). The report of favorable conditions for the occurrence of fires on vegetation cover (CFOI), of the Cajamarca region, determined that, in 2019, 26% of the regional territory presented a high level of conditions conducive to the occurrence of forest fires (SIAR, 2019). The lack of estimates of the severity level of forest fires in the Cajamarca region based on remote sensors and calibrated with field data hinders decision-making by the competent authorities. Therefore, the present research aims to evaluate the severity and post-fire vegetation recovery using satellite images, in order to provide information to decision-makers and assist in the restoration and improvement of damaged areas, while analyzing the behavior of fires in this part of the Peruvian territory.

Methods

Study area

The department of Cajamarca is located in northern Peru, approximately 800 km from the capital, Lima (Fig. 1). It covers an area of 33,317.54 km^2 (Sineace, 2020). Politically, it is divided into the provinces of Cajamarca, Cajabamba, Celendín, Chota, Contumazá, Cutervo, Hualgayoc, Jaén, San Ignacio, San Marcos, San Miguel, San Pablo, and Santa Cruz, with an approximate population of 1,341,012 inhabitants (INEI, 2018).

According to the Ecological and Economic Zoning (ZEE) of the Cajamarca department, 39% of the Cajamarca territory is allocated to productive zones (1,286,576 ha), of which 20.5% corresponds to agriculture (263,762 ha), 19.4% to pasture for livestock (249,596 ha), and 23.7% to forestry production (305,397 ha) (Quispe, 2017). According to the National Meteorology and Hydrology Service (SENAMHI) (https://www.senamhi.gob.pe/), the region has an average annual temperature of 14.7 °C, with average maximum and minimum temperature values ranging between 4.9 and 22.2 °C. The average relative humidity is 72%, and rainfall varies between 380 and 1200 mm per year.

The relief, strongly influenced by the Andes Mountains, conditions agricultural and livestock development according to altitude and soil characteristics (DGP, 2019).

According to CENEPRED (2022), the department of Cajamarca has a high incidence of forest fires, with 42.08% of its territory classified in high and very high risk levels, affecting approximately 1,388,605 hectares. The months of November and December register the highest frequency of occurrence, with the provinces of Jaén, Cajamarca, Cutervo, Celendín, and Chota being considered the most critical.

Methodological approach

Figure 2 shows the methodological process to assess the severity and recovery of post-fire vegetation in the Cajamarca department through the analysis of satellite images and remote sensing. The first step was to identify fires occurring between 2020 and 2021 from hot spot data captured by MODIS and VIIRS sensors, obtained from the FIRMS platform. To determine the levels of extreme, high, medium, and low severity and vegetation recovery for pre-, during, and post-fire, the Normalized Burned Area Ratio (NBR) and Normalized Difference Vegetation Index (NDVI) were applied to analyze fire severity and monitor vegetation regeneration. Over the last two decades, numerous spectral indices have been developed to quantify fire severity, each showing specific strengths in local studies (Guo et al. 2024a, b). Although these indices differ in the combination of spectral bands used, which leads to differences in their performance for assessing severity, the highest accuracy for fire severity classification has been reported for RdNBR (Sentinel) and dNBR (Landsat) (Güney et al. 2023). In this sense, the differenced Normalized Burn Ratio (dNBR) has become the standard spectral index for evaluating fire severity (Guo et al. 2024a, b; Veraverbeke et al. 2012). On the other hand, vegetation indices play an important role in remote sensing studies of burned forest areas and fire severity (Kurbanov et al. 2022). The Normalized Difference Vegetation Index (NDVI), calculated by combining the red and NIR bands, is well correlated with fire severity (Guo et al. 2024a, b; Ryu et al. 2020).

Gathering cartographic information

Data collection was based on records of hot spots detected by MODIS (resolution: 1 km) and VIIRS (resolution: 375 m) sensors in Peru during 2020 and 2021 (Table 1). FIRMS data (downloaded on 03/11/2021, https://firms.modaps.eosdis.nasa.gov/download/), extensively validated for forest fires (Çolak & Sunar 2020; Morresi et al. 2019; Suresh Babu et al. 2016), were complemented with geospatial layers from the MINAM Geoserver (https://geoservidor.minam.gob.pe/recursos/intercambiodedatos/). This integration allowed delimiting

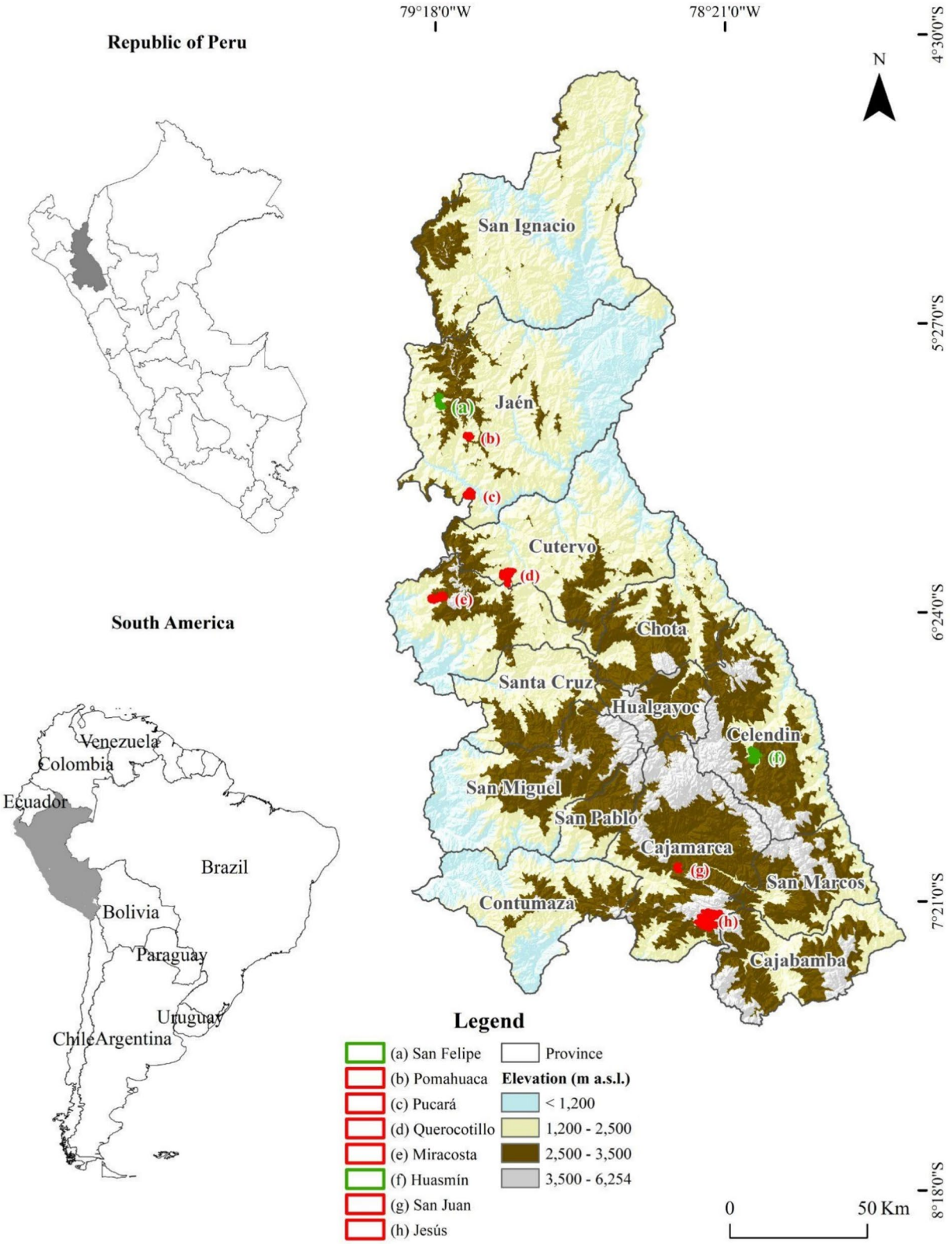

Fig. 1 Location of the study area. Sites (**a**) and (**f**) correspond to fires in forested areas (green symbols), whereas sites (**b**–**e**), (**g**), and (**h**) correspond to fires in areas dominated by shrubs, grasslands, and herbaceous vegetation (red symbols)

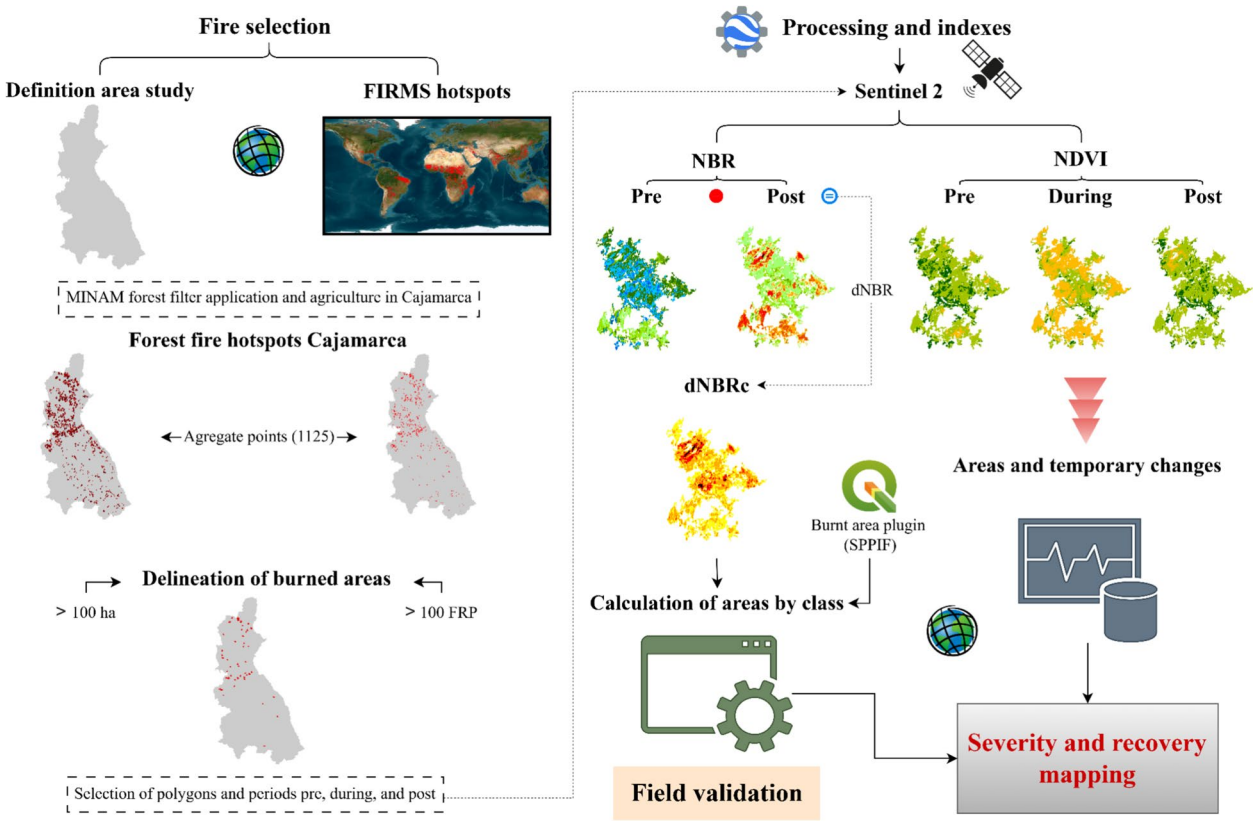

Fig. 2 Methodological diagram for assessing fire severity and post-fire regrowth

Table 1 MODIS and VIIRS hot spots downloaded from FIRMS geoserver

Id	Instrument	Year	Heat sources
fire_nrt_M-C61_199225	MODIS	2021	885
fire_archive_M-C61_199225	MODIS	2020	17,919
fire_nrt_J1V-C2_199226	VIIRS	2020	104,751
fire_nrt_V1_199227	VIIRS	2021	1510
fire_archive_V1_199227	VIIRS	2020	102,567

forest areas excluding urban, agricultural, and aquatic areas, ensuring that only fires in forest areas were analyzed.

MODIS and VIIRS products provide highly relevant information on fire events, their spatial and seasonal trends (Biogeosciences & Alperen Coskuner 2022). MODIS fire products have a nominal spatial resolution of 1 km, which is very low compared to the size of typical forest fire features. However, simulations show that MODIS has a 50% chance of detecting a 100 m^2 (~ 1000 K) flaming fire or a 1000–2000 m^2 smoldering fire (Eckmann et al. 2008; Fraser et al. 2000; Giglio et al. 2016; Hawbaker et al. 2008). Furthermore, algorithms cannot detect fires through dense clouds or smoke. Therefore, a large fire may go undetected for several days and then reappear; a small fire may burn and extinguish without being detected (Fraser et al. 2000). Given the above, smaller fires (< 100 ha) were excluded from this research (Vetrita et al. 2021).

Identification of areas affected by forest fires

The first filter was based on MODIS and VIIRS hot spot extraction using standardized methods (Li et al. 2018; Yang et al. 2023). These data were intersected with Cajamarca boundaries using QGIS 3.28 and checked against local GeoMINAM records to exclude urban, agricultural, and aquatic areas. The second filter, applied with a MIDAGRI agricultural layer, reduced the initial foci, retaining only those in forested areas. Finally, the perimeters of burned areas were delimited. For this purpose, size and heat intensity criteria were established (González-Gutiérrez et al. 2020; Vilchis-Francés et al. 2015) that allowed the identification of significant fires, ensuring that the analysis focused on ecologically relevant events:

– Size: perimeters of forest fires with areas larger than 100 ha were estimated.
– Heat intensity: heat sources with normalized Fire Radiative Power (FRP) ≥ 100 MW/km^2 were selected using Eq. 1:

$$FRP(n) = FRP/(SCAN * TRACK) \quad (1)$$

Where:

- FRP(n): normalized Fire Radiative Power (MW/km.^{2})
- FRP: measured Fire Radiative Power (MW/pixel)
- SCAN: satellite perpendicular scan width (km)
- TRACK: satellite sampling orbital path length (km)

Determination of severity level in forest fires

Fires with an affected area greater than 100 hectares were subjected to a selection process by applying inclusion and exclusion criteria. Heat intensity was estimated from active hot spot data obtained from MODIS and VIIRS sensors. For each active-fire pixel, we calculated the normalized Fire Radiative Power FRP(n) (MW km^{-2}) using Eq. (1). Hotspots with FRP(n) ≥ 100 MW km^{-2} were then grouped into spatial clusters through a kernel analysis of FRP values, and clusters that met the criteria of burned area > 100 ha and presence of high-intensity pixels were retained as individual fire events. This procedure allowed us to accurately identify high-energy fires and robustly delimit their spatial extent.

Pre-fire and post-fire dates were determined from the chronological analysis of forest hot spots detected for each cluster, identifying the first and last record of the event. In order to capture pre-fire and post-fire conditions more accurately, the start date was set as the day before the first heat thermal anomaly and the end date as the day after the last active record (Briones-Herrera et al. 2020).

The satellite images were processed using the GEE platform, in which a script developed by Silva-Cardoza et al. (2022) was adapted and applied, modified to incorporate specific dates corresponding to the periods before, during, and after each fire. The necessary spectral indices to quantify the changes in the vegetation caused by the fire and to delimit the burned areas were calculated from these images (Escuin et al. 2008).

The corrected Differential Normalized Burning Index (dNBRc) was used to determine the severity of the fire (Silva-Cardoza et al. 2022). It was obtained by the difference between the values of the NBR derived from multispectral images captured for the pre- and post-fire periods. The name dNBRc refers to the application of a phenological correction, as detailed in Briones-Herrera et al. (2020), with the purpose of minimizing natural seasonal variations in vegetation that could interfere in the interpretation of changes attributable to fire.

For the spatial analysis and cartographic representation, ArcGis 10.8 software was used. The burned areas were classified into severity levels (low, medium, high, and extreme) using a symbology adapted to the conditions of the study area. This classification was based on the ranges established by Briones-Herrera et al. (2022) for the values of spectral indices and was supported by the files and criteria of the Mexican Forest Fire Danger Prediction System (SPPIF) (http://forestales.ujed.mx/incendios2/#). The symbology was modified to suit the ecological context of the region of analysis, thus ensuring a consistent interpretation of fire impacts on vegetation. The color ramp of the symbology established colors: yellow, representing low damage; orange, medium damage; red, high damage; and black, extreme damage (Briones-Herrera et al. 2022). The Burned Area Plugin downloaded from SPPIF and compatible with QGis 3.16.11 was used to map the perimeter of the fires.

Based on the dNBRc thresholds proposed by Silva-Cardoza et al. (2021) for temperate forests, we visually inspected the dNBRc histograms and spatial patterns of the eight fires and compared them with the severity observed in the field in the two validated fires. The original thresholds used in this study were unburned < 66, low severity 66–197, medium severity 197–394, high severity 394–590, and extreme severity > 590 (dNBRc units scaled by 10^3) (Table 2).

Using the GEE platform, Sentinel-2 MSI Level 2 A surface reflectance images (COPERNICUS/S2_SR collection) were downloaded and processed for the periods before and after the fire for each event. From these scenes, the NBR was calculated using the 20 m 8 A (NIR) and 12 (SWIR) resolution bands. Subsequently, the dNBR was obtained from the temporal difference in NBR between the scenes before and after the fire (Delcourt et al. 2021). Finally, the dNBRc was derived by applying a phenological correction, with the aim of improving the accuracy of fire severity detection. For each fire, the dNBRc was determined by calculating the average value of dNBR in all pixels located from 3 to 5 km outside the fire perimeter (Briones-Herrera et al. 2022). Once the images were processed and reclassified using the dNBRc index, the areas where the intensity of the fire affected the ecosystem were verified using orthophotos. This remote verification was complemented by exhaustive field work, in order to validate the results obtained by remote sensing.

During the satellite analysis, a total of eight forest fires were identified in the study area. Of these events, two representative fires were selected for field verification,

Table 2 Fire severity classification according to dNBRc values for temperate ecosystems

Severity	Classification values (*)
Unburned	< 66
Low	66–197
Medium	197–394
High	394–590
Extreme	> 590

(*) Classification thresholds correspond to dNBRc values calculated from NBR scaled by 10^3 and stored as integer values, according to Lutes et al. (2006)

Table 3 Severity levels in vegetation according to the percentage of scorching in the canopy

Vegetation severity level	Description
Unburned (control)	Unburned tree crown
Low	Crown scorch < 1/3 of the tree crown
Medium	Crown scorch > 1/3 and < 2/3 of the tree crown
High	Crown scorch > 2/3 and < 90% of the tree crown
Extreme	Crown consumption > 90% of the tree crown

considering their accessibility, magnitude, and diversity of spectral severity levels classified as follows.

The second step consisted of evaluating fire severity in the field; for this purpose, 10 plots were identified and selected (two plots with a radius of 9 m and eight plots with a radius of 15 m) systematically distributed in areas representative of the different severity levels previously classified. Then, three transects were established in each plot, where in each transect three 30 × 30 cm square sampling subsites were identified (Gonzáles et al. 2024; Morfin-Ríos et al. 2012; Silva-Cardoza et al. 2021). The geographic location of the plots was recorded using a Global Positioning System (Garmin GPSmap 79S), which allowed georeferencing and comparison with the results derived from the satellite analysis.

In each plot, the following severity variables were evaluated in the field:

- Percentage of vegetation cover affected
- Level of soil and litter carbonization
- Damage to tree and shrub canopy foliage
- Presence of post-fire regrowth
- Mortality of herbaceous and woody species

The in situ severity level was assigned based on a standardized visual key proposed by Silva-Cardoza et al. (2021), which classifies severity into five levels: not burned, low, medium, high, and extreme. Table 3 contains the measures of vegetation severity levels according to the percentage of crown affected by fire.

Among the eight mapped fires, we selected the Huasmín and San Felipe events for field validation because they combined (i) contrasted severity gradients, (ii) accessibility and safety conditions, and (iii) representativeness of the dominant fuel types in the region. In total, 10 circular plots (2 plots with 9 m radius and 8 plots with 15 m radius) were distributed across the five dNBRc severity classes (unburned, low, medium, high, and extreme), following the procedure described by Silva-Cardoza et al. (2021). For each plot, we assigned a field-based severity class and extracted the corresponding dNBRc class from the map.

Verification of post-fire natural regeneration indicators

To evaluate post-fire vegetation recovery, a script was developed in the GEE platform, using the NDVI formula proposed by Rouse et al. (1973), as shown in Eq. 2:

$$NDVI = (NIR - RED)/(NIR + RED) \quad (2).$$

Where:

- NDVI is the Normalized Difference Vegetation Index on a scale of −1 to 1.
- NIR is the light reflected in the near-infrared spectrum.
- RED is the reflected light in the red range of the spectrum.

Of the eight fires evaluated, two occurred in forested areas and six in areas dominated by scrubland, grassland, and herbaceous vegetation. For this reason, field validation was carried out only in the two forested areas, where it was possible to more accurately assess the severity levels in the tree cover, in accordance with the criteria established in the study.

The analysis was carried out using satellite images from the Sentinel-2 sensor, corresponding to three key moments: before the fire (approximately 2 months before the event), during the fire, and after the fire (approximately 3 months after the event). Due to the high cloud cover in the study area, cloud cover of less than 30% was considered in order to obtain clear images for the study areas.

The three key moments of analysis in this study are shown in Table 4.

For the general analysis of vegetation cover, composites based on the median of Sentinel-2 images were used, which allowed minimizing the influence of outliers and generating a more stable representation of the spectral

Table 4 Download dates of the Sentinel-2 images used for the NDVI analysis of the fire

Fire	Fecha_pre	Fecha_dur	Fecha_post
Huasmín	'2020–05–25', '2020–08–25'	'2020–09–26', '2020–11–30'	'2020–12–30', '2021–03–30'
Jesús	'2020–04–21', '2020–07–21'	'2020–08–22', '2020–11-03'	'2020–12-03', '2021–03-03'
Miracosta	'2020–06-06', '2020–09-05'	'2020–10-04', '2020–11–20'	'2020–12–20', '2021–03–20'
Pomahuaca	'2020–05–10', '2020–08–10'	'2020–09–10', '2020–11-09'	'2020–12-09', '2021–03–09'
Pucará	'2020–06–28', '2020–09–28'	'2020–10–27', '2020–12–28'	'2021–01–28', '2021–04–28'
Querocotillo	'2020–04–18', '2020–07–18'	'2020–08–18', '2020–10-06'	'2020–11-06', '2021–02–06'
San Felipe	'2020–06–30', '2020–09–30'	'2020–10–30', '2020–11–30'	'2020–12–30', '2021–03–30'
San Juan	'2020–05–20', '2020–08–25'	'2020–09–25', '2020–10–25'	'2020–11–25', '2021–02–25'

Table 5 NDVI classification according to vegetation type

Class	Type of vegetation
−1–0	Sparse vegetation or bare soil
0–0.33	Vegetation with some type of deficiency
0.33–0.66	Moderately healthy vegetation
0.66–1	Very healthy vegetation

behavior of the landscape. Additionally, post-fire visual mosaics were generated to facilitate the spatial interpretation of recovery patterns.

Once the NDVI images were generated, we proceeded to their analysis within ArcGIS 10.8 software, where NDVI values were reclassified according to the proposal of Filicetti et al. (2018), in order to evaluate the quality of the post-fire vegetation cover, as detailed in Table 5.

Results

Identification of areas affected

A total of 366,060 hot spots were recorded in Peru, detected by MODIS and VIIRS sensors. Of these, 9077 hot spots corresponded to the Cajamarca department with occurrences in primary forest, secondary forest, grasslands, agricultural areas, and pastures. When applying the MINAM forest layer filter, non-forest outbreaks were discarded, resulting in 4949. Subsequently, when filtering with the agricultural use layer of the region, 1795 outbreaks located in agricultural areas were identified; the difference of 3154 remaining outbreaks corresponded to detections in forest areas (210 from MODIS and 2944 from VIIRS).

From the 3154 forest hot spots, 351 clusters were generated with areas ranging from 0 to 648 ha, for a total of 17,251 ha throughout Cajamarca. Of these clusters, 48 exceeded 100 ha and 101 had a Fire Radiative Power (FRP) greater than 100 MW/km^2. Crossing both criteria (area > 100 ha and FRP > 100) resulted in a subset of 32 clusters, from which eight representative fires were selected, named according to the place of occurrence: San Felipe, Pucará, Pomahuaca, Miracosta, Huasmín, San Juan, Jesús, and Querocotillo. The selection was based on the presence of trees, accessibility (topographic and social considerations), and the visibility of signs of the fire.

Determination of the severity level

The NBR index in before and after images for the fires revealed significant differences in the distribution of fire damage. Figure 3 shows the results of the NBR index for the images obtained before and after the eight fires analyzed, showing a marked difference in vegetation when comparing pre-fire and post-fire conditions. In the pre-fire images, blue and green coloration can be seen, indicating that the vegetation has not been affected by the fire, while in the post-fire images the scar left by the impact of the fire on the vegetation is evident, generating pixels with dark tonality that represent less recovery of the vegetation. Thus, it is evident to appreciate the scar left by the impact of fire in the Pomahuaca, Pucará, and San Juan fires, since the entire surface shows a marked dark coloration. In contrast, the fires in San Felipe, Querocotillo, Miracosta, Huasmín, and Jesús show a higher concentration of light pixels, which denotes a recovery in the reflectance of the vegetation due to the growth of some plants that emerged after the rains.

The results of the dNBRc index for the fire incidence areas in the department of Cajamarca are presented in Fig. 4, where, associated with a color symbology (yellow, orange, red, and black) that reflects severity levels (low, medium, high, and extreme), they show the level of affectation during the fire. Accordingly, it is possible to visually differentiate the separation of the index values that classify the severity levels. It is observed that in the eight fires there is a similar pattern of the area burned by the fire, where the most affected areas are surrounded by areas of medium severity followed by low severity, present in most of the affected polygons.

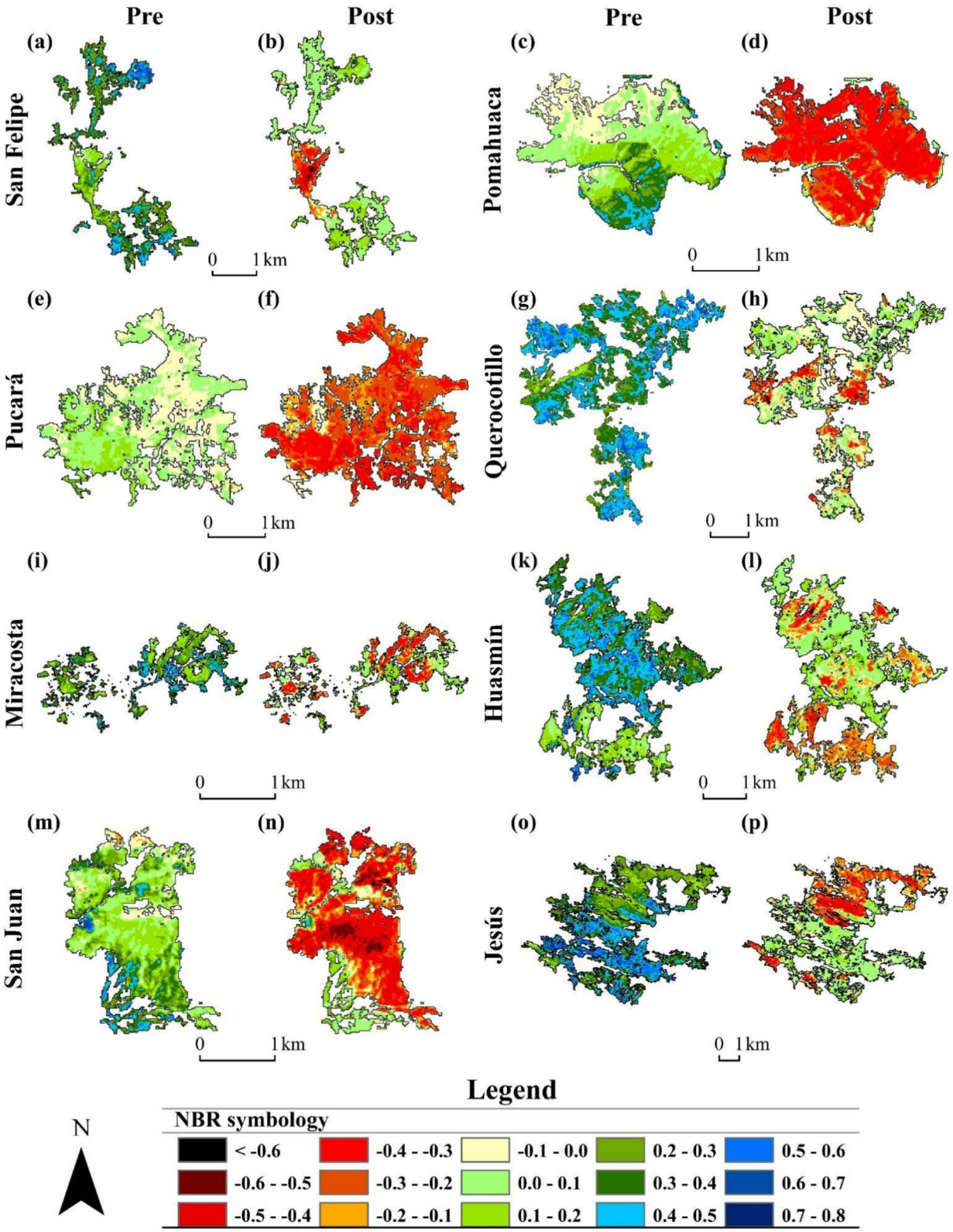

Fig. 3 NBR index (pre-fire and post-fire)

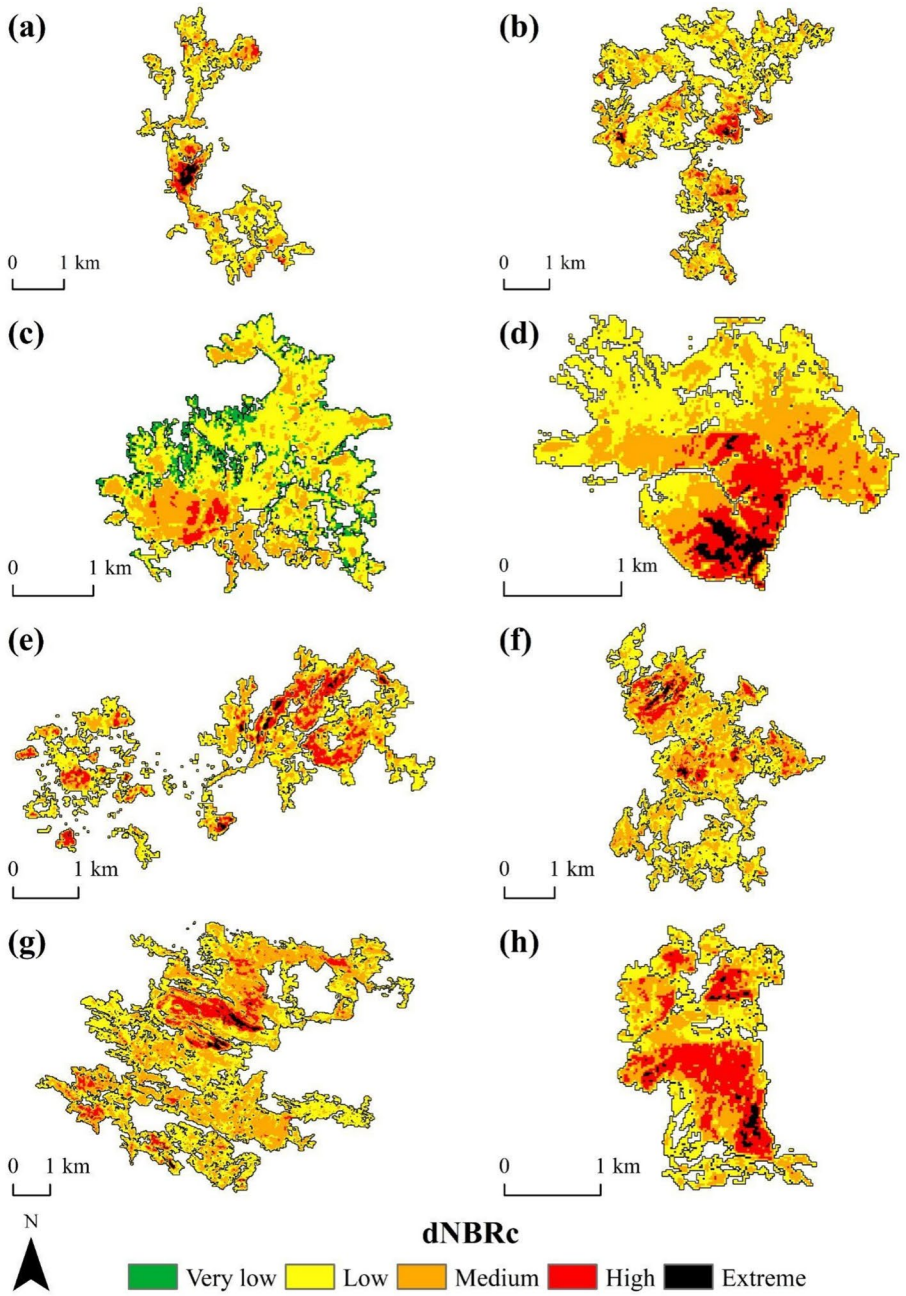

Fig. 4 Severity levels determined by the bitemporal spectral index (before and after the fire) dNBRc of the fires distributed in five provinces of the Cajamarca region: in the province of Jaén there are the San Felipe, Pomahuaca, and Pucará fires (**a**, **b**, and **c**), in the province of Cutervo the Querocotillo fire (**d**), in the province of Chota the Miracosta fire (**e**), in the province of Celendín the Huasmín fire (**f**), and in the province of Cajamarca the San Juan and Jesus (**g** and **h**)

In aggregate terms, the total area impacted by the eight fires amounted to 6028.06 ha. Low severity predominated with 4278.60 ha (71.02% of the total), followed by medium severity with 1323.33 ha (21.95%), high severity with 386.69 ha (6.41%), and extreme severity with 39.44 ha (0.65%) (Table 6).

On a specific scale, the fire in Jesús was particularly noteworthy for being the largest, with 2422.48 ha affected, mainly in the low severity category (74.90% of the area). On the other hand, San Felipe and Huasmín had relatively smaller affected areas (345.30 ha and 793.06 ha, respectively), with a predominance of low

Table 6 Area affected by fires according to severity level of the dNBRc index

Fire	Total area	Severity			
	ha	Low (ha)	Medium (ha)	High (ha)	Extreme (ha)
San Felipe	345.30	279.21	39.97	16.40	9.71
Huasmín	793.06	566.74	183.24	36.57	6.51
Jesús	2422.48	1814.44	475.16	132.84	0.04
Miracosta	452.92	259.10	149.59	40.85	3.38
Pomahuaca	354.36	150.16	137.48	55.12	11.60
Pucará	535.36	350.64	169.12	15.60	0.00
Querocotillo	845.95	749.96	69.49	23.55	2.95
San Juan	278.64	108.36	99.28	65.76	5.24
Total	6028.06	4278.60	1323.33	386.69	39.44

severity and few areas of extreme severity. The Pomahuaca fire stands out for the greater relative proportion of high (55.12 ha) and extreme (11.60 ha) severity areas compared to its total area (354.36 ha), while Querocotillo showed a high predominance of lightly affected areas (94.15% with low severity).

Finally, San Juan, with the smallest total area affected (278.64 ha), stood out for having a more balanced distribution between low, medium, and high severity categories.

Verification of indicators of natural regeneration

The temporal evaluation of the NDVI index made it possible to determine the state of the vegetation cover before, during, and after the forest fires that occurred in the department of Cajamarca. The results show that vegetation health and activity were affected during the fire, followed by a variable recovery in the post-fire period, determined by the edaphoclimatic conditions of each site.

In the pre-fire period, vegetation cover predominated in the moderately healthy (NDVI between 0.33 and 0.66) and very healthy (NDVI > 0.66) vegetation classes. In Huasmín, 95.90% of the area presented NDVI values higher than 0.33, distributed in 74.61% of moderately healthy vegetation and 21.29% classified as very healthy. During the fire, the very healthy category was reduced to 3.40%, while the poor vegetation (NDVI between 0 and 0.33) increased to 59.18%. In the post-fire period, moderately healthy vegetation dominated (80.53%), and very healthy cover accounted for 14.89% of the area. In Jesús, very healthy vegetation decreased from 27.85% pre-fire to 9.69% during the fire and 6.70% in the post-fire period, whereas the moderately healthy category remained predominant, varying from 65.67% pre-fire to 66.27% post-fire. In Pomahuaca, the behavior was more drastic: during the fire, 87.48% of the area was classified as deficient, but this condition partially reversed in the post-fire period, when moderately healthy vegetation reached 59.79% and poor vegetation decreased to 39.08%. Highly positive responses were observed in Pucará and San Felipe. In Pucará, very healthy vegetation increased from 0.11% pre-fire to 41.26% post-fire, accompanied by a marked reduction of vegetation with some type of deficiency from 49.60% to 1.04%. In San Felipe, very healthy vegetation rose from 14.83% pre-fire to 53.11% post-fire (21.57% during the fire). In San Juan, on the other hand, recovery was slower, with 36.00% of the area still classified with low NDVI after the fire, despite registering 59.10% of moderately healthy cover and only 4.90% of very healthy cover.

These results reflect a significant recovery in most of the evaluated sites; however, this did not follow the same behavior, since marked differences were observed from one site to another. Detailed NDVI values for each vegetation cover class in the pre-, during, and post-fire periods are presented in Table 7, providing a quantitative picture of vegetation impact and recovery by locality.

NDVI variation for fires

Table 8 shows the behavior of NDVI for the fire areas evaluated in three time periods (pre-, during, and post-fire) allowing the identification of clear quantitative patterns of vegetation impact and recovery. The comparison between times shows that all fires experienced deterioration in vegetation health during the fire, with marked differences in the magnitude of the impact and in the recovery response.

In the Miracosta and Querocotillo fires, NDVI was moderately reduced during the fire, decreasing from 0.58 to 0.45 and from 0.57 to 0.52, respectively; however, post-fire mean values remained below their initial levels (0.42 and 0.36). On the other hand, in Pomahuaca and Pucará, NDVI was reduced to low levels during the fire (0.22 and 0.21, respectively), but subsequently showed marked increases (0.36 and 0.63, respectively), reflecting a stronger recovery response. San Felipe showed one of the greatest post-fire recoveries, with a mean NDVI of 0.62, exceeding its pre-fire value (0.50). In contrast, San Juan presented a post-fire NDVI of only 0.39, indicating a slower and more limited recovery.

The analysis of the coefficient of variation (CV) reveals that during the fires, NDVI heterogeneity increased in all sites, and although this trend generally decreased after the event, post-fire CV values in some areas remained

Table 7 NDVI values according to range threshold for pre-, during, and post-fire times

Fire	Type of vegetation	Evaluation time					
		Pre		During		Post	
		ha	%	ha	%	ha	%
Huasmín	Bare soil	0.00	0.00	0.00	0.00	0.00	0.00
	With some deficiency	32.60	4.11	469.72	59.18	36.32	4.58
	Moderately healthy	592.20	74.61	297.08	37.43	639.24	80.53
	Very healthy	168.96	21.29	26.96	3.40	118.20	14.89
Jesús	Bare soil	0.00	0.00	0.00	0.00	0.00	0.00
	With some deficiency	156.84	6.47	805.84	33.27	654.72	27.03
	Moderately healthy	1590.96	65.67	1382.00	57.05	1605.40	66.27
	Very healthy	674.68	27.85	234.64	9.69	162.36	6.70
Miracosta	Bare soil	0.00	0.00	0.00	0.00	0.00	0.00
	With some deficiency	10.04	2.21	130.04	28.58	146.00	32.09
	Moderately healthy	320.44	70.42	266.68	58.61	262.32	57.65
	Very healthy	124.56	27.37	58.32	12.82	46.72	10.27
Pomahuaca	Bare soil	0.00	0.00	0.00	0.00	0.00	0.00
	With some deficiency	81.08	22.88	310.00	87.48	138.48	39.08
	Moderately healthy	254.68	71.87	41.40	11.68	211.88	59.79
	Very healthy	18.60	5.25	2.96	0.84	4.00	1.13
Pucará	Bare soil	0.00	0.00	0.00	0.00	0.00	0.00
	With some deficiency	265.52	49.60	493.16	92.12	5.56	1.04
	Moderately healthy	269.24	50.29	42.16	7.88	308.92	57.70
	Very healthy	0.60	0.11	0.04	0.01	220.88	41.26
Querocotillo	Bare soil	0.00	0.00	0.00	0.00	0.12	0.01
	With some deficiency	16.48	1.94	40.72	4.80	368.48	43.39
	Moderately healthy	669.08	78.79	705.92	83.13	459.60	54.12
	Very healthy	163.64	19.27	102.56	12.08	21.00	2.47
San Felipe	Bare soil	0.00	0.00	0.12	0.03	0.00	0.00
	With some deficiency	37.56	10.83	85.72	24.71	36.60	10.55
	Moderately healthy	257.92	74.35	186.24	53.68	126.08	36.34
	Very healthy	51.44	14.83	74.84	21.57	184.24	53.11
San Juan	Bare soil	0.00	0.00	0.00	0.00	0.00	0.00
	With some deficiency	5.92	2.12	189.96	68.17	100.32	36.00
	Moderately healthy	188.64	67.70	82.56	29.63	164.68	59.10
	Very healthy	84.08	30.18	6.12	2.20	13.64	4.90

1: sparse vegetation or bare soil; 2: vegetation with some type of deficiency, 3: moderately healthy vegetation, and 4: very healthy vegetation

above pre-fire levels, indicating spatially heterogeneous regeneration.

The analysis of the rate of variation (TV) of NDVI reveals a rapid degradation of vegetation caused by fire and a differential recovery behavior between fires. The pre → during transition shows negative values in all sites, evidencing an effect of vegetation degradation after fire impact. The most pronounced reductions were recorded in San Juan (−48.52%), Pomahuaca (−47.32%), and Huasmín (−39.87%), which reflects a notable effect on the active vegetation cover. However, the during → post transition revealed a positive and accelerated vegetation response in several study areas. Pucará (199.31%) and Pomahuaca (64.37%) showed the highest recovery rates, followed by San Juan (33.19%) and San Felipe (26.41%), whereas Jesús (2.29%) exhibited only slight improvement and Miracosta (−5.66%) and Querocotillo (−29.94%) continued to decline. The final pre → post balance reveals that only Pucará (+85.98%) and San Felipe (+23.31%) managed to exceed the pre-fire vegetation state in terms of NDVI, while the remaining sites did not reach their initial values, particularly Querocotillo (−35.96%), San Juan (−31.43%), and Miracosta (−26.66%). This contrast suggests ecosystem variability in both regeneration

Table 8 Statistical values of NDVI for the study areas at different times

Fire	Stage	Mean	SD	CV (%)
Huasmín	Pre	0.55	0.13	23.67
	During	0.33	0.16	47.31
	Post	0.53	0.12	22.14
Jesús	Pre	0.56	0.15	26.9
	During	0.42	0.15	34.9
	Post	0.43	0.15	34.53
Miracosta	Pre	0.58	0.12	20.72
	During	0.45	0.17	38.59
	Post	0.42	0.18	41.58
Pomahuaca	Pre	0.42	0.13	31.59
	During	0.22	0.11	48.67
	Post	0.36	0.1	27.16
Pucará	Pre	0.34	0.07	20.52
	During	0.21	0.08	37.04
	Post	0.63	0.1	16.23
Querocotillo	Pre	0.57	0.1	18.05
	During	0.52	0.12	22.64
	Post	0.36	0.13	35.98
San Felipe	Pre	0.5	0.15	28.74
	During	0.49	0.21	43
	Post	0.62	0.2	31.43
San Juan	Pre	0.57	0.13	23.11
	During	0.3	0.15	50.97
	Post	0.39	0.13	33.7

Table 9 Rate of change of NDVI for the study areas at different times

Fire	Comparison	ΔNDVI (%)
Huasmín	Pre → during	−39.87
	During → post	61.09
	Pre → post	−3.14
Jesús	Pre → during	−24.42
	During → post	2.29
	Pre → post	−22.69
Miracosta	Pre → during	−22.25
	During → post	−5.66
	Pre → post	−26.66
Pomahuaca	Pre → during	−47.32
	During → post	64.37
	Pre → post	−13.41
Pucará	Pre → during	−37.86
	During → post	199.31
	Pre → post	85.98
Querocotillo	Pre → during	−8.6
	Durante → post	−29.94
	Pre → post	−35.96
San Felipe	Pre → during	−2.46
	During → post	26.41
	Pre → post	23.31
San Juan	Pre → during	−48.52
	During → post	33.19
	Pre → post	−31.43

capacity and post-fire functional efficiency. A detailed summary of the NDVI rate of variation across all sites and time intervals is presented in Table 9, supporting the observed spatiotemporal dynamics.

The temporal variation (before-pre, during) and vegetation recovery after fires (post) in the eight study sites (San Felipe, Pomahuaca, Pucará, Querocotillo, Miracosta, Huasmín, San Juan, and Jesús) is shown in Fig. 5. The spatial representation of the Normalized Difference Vegetation Index (NDVI) levels allows us to identify the differential impact of the fires in each study site and the degree of vegetation recovery. In all cases, a decrease in NDVI was observed during the fires, evidenced by the expansion of red and orange areas, indicating loss of vegetation cover. In the "post" stage, localities such as San Juan (Fig. 5u), Jesús (Fig. 5x), and Querocotillo (Fig. 5i) show partial recovery, reflecting a limited or slow regeneration (Table 7); on the contrary, San Felipe (Fig. 5c) and Huasmín (Fig. 5r) show a marked recovery of greenness in the "post" stage, with a greater presence of light and dark green shades compared to during the fire.

The NDVI values reveal that, in San Felipe, mean NDVI changed from 0.50 before the fire to 0.49 during the fire and increased to 0.62 post-fire, accompanied by an expansion of the very healthy vegetation class (NDVI > 0.66) from 14.83% to 53.11% of the burned area. With respect to Huasmín, mean NDVI decreased from 0.55 to 0.33 during the fire ($\Delta = -0.22$), a trend that was repeated in all study sites, as all forest physiognomies showed a marked decrease in NDVI during the fire, even in unburned areas.

Discussion

The evaluation of severity and post-fire vegetation recovery was based on cartographic information of hot spots and the processing of Sentinel-2 satellite images, which made it possible to accurately identify the location, magnitude, and spatial behavior of forest fires in the Cajamarca region. As stated by Añamuro-Luque et al. (2020), tools based on geographic information systems and remote sensing are useful for mapping burned areas, identifying fire severity and monitoring vegetation regeneration.

In this study, the selection of fires was carried out under criteria adjusted to the regional context: clusters larger than 100 ha and FRP greater than 100 MW/km^2.

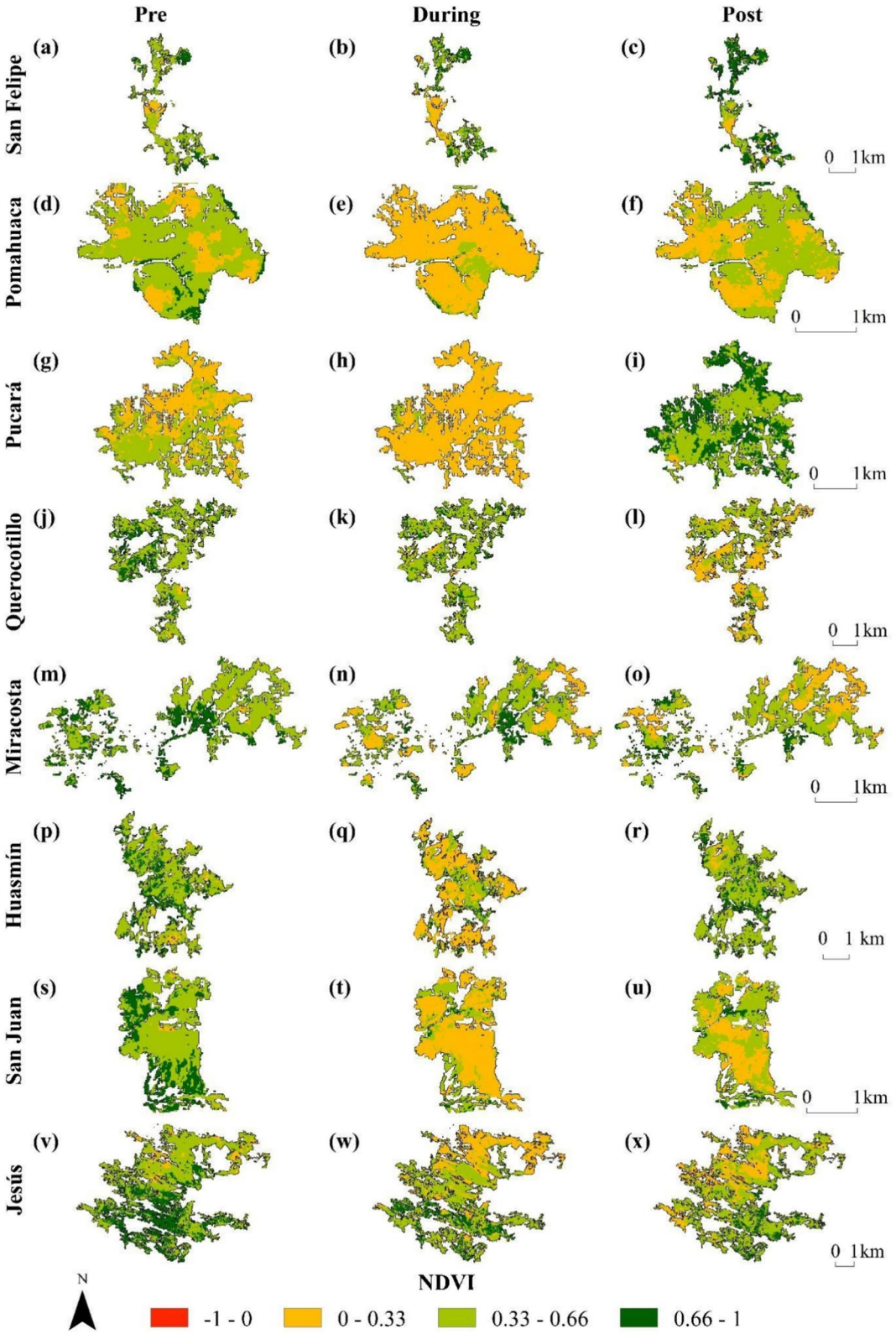

Fig. 5 Spatiotemporal variation of the Normalized Difference Vegetation Index (NDVI) in areas affected by forest fires in eight localities of the Cajamarca region—Peru, at three points in time (pre-, during, and post-fire)

Although other authors, such as Gómez-Sánchez et al. (2017), define large fires as those larger than 500 ha, the adaptation of this category was justified by the predominance of smaller events in the Cajamarca region, which despite their size cause the same damage, affecting the connectivity and resilience of ecosystems and implying serious consequences for ecology, the environment, the population, and property (Kala 2023). The disruption of local economies due to forest fires directly affects the livelihoods of small farmers (Carmo et al. 2022), whose incomes often require greater dependence on the sustainable exploitation of available natural resources to increase their income (Lopes et al. 2025).

An important factor influencing hotspot detection is the temperature thresholds of fire candidates (Kumar & Kumar 2022). In thermal remote sensing, thresholds determine the level at which a pixel is classified as a fire candidate. Lower thresholds will allow smaller fires to be detected with a lower average temperature of the fire pixel (Qian et al. 2009). However, lower thresholds for selection would result in a strong overestimation of fires, especially in areas with a warmer background > 300 K, such as small urban areas and bare soils that are not detected with exclusion masks or filters (Plank et al. 2017). Conversely, the corresponding MODIS channel saturates at approximately 500 K (Justice et al. 2002), which favors the use of higher thresholds and allows the selection of fire candidates in areas with warmer backgrounds. Therefore, in fire detection with MODIS data, the detection work is mainly based on infrared bands sensitive to ground temperature, to detect abnormally high temperature points on the ground according to the fixed brightness temperature threshold (Ding et al. 2023). In this research, the co-regulated dNBR index (dNBRc) was used to classify severity, using the threshold values proposed by Silva-Cardoza et al. (2021) for temperate forests, which are the result of applying statistical models to predict severity assessment in the field in temperate forest ecosystems (pine, pine-oak, oak-pine). Unlike the thresholds defined by Key and Benson (2006), which were formulated for the dNBR index without phenological correction, the methodology adopted in this study incorporates a seasonal correction that improves the detection of changes attributable to fire. As part of the procedure, we visually inspected the histograms and spatial patterns of dNBRc for the eight fires analyzed and compared them with the severity observed in the field in the two validated fires. In other words, the remote indices (RBRc, dNBRc) were calibrated with actual observations of vegetation and soil severity. This approach allowed us to adjust the severity ranges to the structural and functional characteristics of the areas evaluated in the Cajamarca region and confirm that the ranges proposed by Silva-Cardoza et al. (2021) were consistent with the spectral distribution and observations of vegetation and soil damage in the study area.

The results obtained reveal that most of the fires evaluated had medium to low severity levels, which is consistent with Fernández-García et al. (2019), who argue that these patterns may be associated with the type of vegetation and its degree of structural maturity, as well as with its natural fire regime. On the other hand, other research has explained the factors that influence the severity of fires; Estes et al. (2017) documented that topography, climate, and fuels are known factors that drive fire behavior; for example, fires on high and middle slopes tend to burn more severely than low slopes; and east and southeast orientations tend to burn more severely than other orientations. Shrub vegetation was also more likely to burn more severely than mixed hardwood/coniferous or hardwood vegetation (Stevens-Rumann et al. 2020). This background information allows us to understand that the predominantly low to medium levels observed in the study area may be associated with both the structural characteristics of the vegetation and the interaction between topographic and environmental factors, which may influence fire behavior, given that the study areas are dominated by shrub vegetation and pine plantations. and its relief is strongly influenced by the Andes Mountain range, which conditions agricultural and livestock development due to the altitude and soil characteristics.

The spatial distribution of severity showed a concentric pattern, with the most severely affected areas located at the core of the fires, surrounded by areas with moderate and low damage. The behavior of the NDVI index over time allowed us to identify different regeneration trends. Indeed, Ibarra-Bonilla et al. (2024) revealed that NDVI and SAVI are the most useful spectral indices for assessing post-fire vegetation dynamics. In particular, the NDVI serves as an indicator of vegetation growth and ecosystem change (Nemani et al. 2003; Zahabnazouri et al. 2025) and is the most widely used index for assessing vegetation health and density (Pettorelli et al.,2011). While it is true that time series of indices such as NDVI are influenced by climate and surface changes, as well as being vulnerable to atmospheric effects and different acquisition angles (Corner et al. 2003; Santana 2018); however, the application of data masking techniques using convolution allows the influence of noise to be effectively represented (Corner et al. 2003; Zewdie et al. 2017); as well as in the detection of changes using regression methods, temporal autocorrelation, or nonparametric methods such as the Mann–Kendall test (Forkel et al. 2013; Santana 2018).

The behavior of the NDVI index over time allowed us to identify differentiated regeneration trends. At

the San Felipe and Huasmín sites, significant increases in post-fire NDVI were recorded, reaching values above 0.5, indicating an outstanding recovery. These results coincide with those reported by Spadoni et al. (2020) and Vlassova et al. (2016), who identified values between 0.6 and 0.7 in mountain ecosystems after fire events, which reinforces the hypothesis of high plant resilience in these environments. In contrast, San Juan presented a limited recovery: although NDVI increased from 0.30 to 0.42 after the fire, it failed to recover its pre-fire value (0.57), with a net negative variation of − 26.62%. This behavior suggests a lower regrowth capacity, possibly associated with restrictive edaphoclimatic factors or greater fire severity at the site (Capador et al. 2021).

These contrasted regeneration patterns can be partially explained by environmental and ecological factors. The differences observed in post-fire recovery trajectories among the study sites may be associated with environmental factors that play a decisive role in vegetation resilience. Several studies indicate that resprouting capacity, vegetation structure, and post-fire moisture availability strongly influence the speed of recovery (Mallikarjun et al. 2025; Ouattara et al. 2025), which may explain the higher NDVI increases documented in Pucará and San Felipe, where a rapid transition toward moderately healthy and very healthy vegetation cover was evident. In contrast, the limited recovery observed in Querocotillo, Miracosta, and San Juan may be related to the influence of topographic gradients that modify water availability and solar exposure (Haney et al. 2008; Tangney et al. 2022; Zahura et al. 2024). Likewise, previous research has shown that variability in precipitation, soil moisture retention, and plant functional traits are key determinants of vegetation reestablishment (Xie et al. 2025). These elements highlight the need to integrate edaphoclimatic and vegetation-related variables in future studies to deepen the understanding of the mechanisms that regulate post-fire recovery in high Andean regions.

On the other hand, NDVI values reflected the dynamics of vegetation recovery after a forest fire. When comparing the different moments, it was highlighted that very healthy vegetation recovered more significantly in several sites. In parallel, vegetation with some type of deficiency was reduced, showing a considerable improvement (Table 7), suggesting a general improvement in the functional status of the vegetation cover. This behavior is especially evident in sites such as Pucará and San Felipe, where very healthy vegetation represented up to 18.54% and 71.85% of the total area evaluated, respectively, after the fire. These findings coincide with those reported by Vales et al. (2020), who emphasize the usefulness of these results for urgent decisions, monitoring, and restoration planning, in order to prioritize future actions.

Although this study demonstrates the use of remote sensing techniques to spatially and temporally evaluate the impact of forest fire severity on vegetation, some limitations of the work include the low spatial resolution of the sensor used, as well as the availability of cloud-free satellite images that condition the temporal and spatial selection of the dates of analysis, which could influence the accuracy of the NDVI and dNBRc estimation. Likewise, although field validation was performed, it was restricted to two representative fires, limiting the extrapolation of the results to the entire region. In addition, complementary environmental variables (e.g., precipitation, slope, soil texture) that could have better explained the variability in post-fire response were not incorporated.

It is recommended that future research integrate predictive models of vegetation recovery using machine learning techniques, including longer time series and validation at a larger number of sites. Additionally, the use of radar data such as multispectral Sentinel-1 SAR images can be integrated. Furthermore, it would be valuable to incorporate ecological and socio-environmental variables to better understand the factors that condition vegetation cover regeneration.

Conclusions

This study integrated FIRMS hotspot data with Sentinel-2 imagery and calibrated dNBRc indices to identify and characterize forest fires in Cajamarca, enabling precise mapping of fire severity and improved understanding of its spatial behavior. The results showed that most affected areas exhibited low to medium severity (71.02% and 21.95%, respectively), while high and extreme severity zones represented only a small fraction of the total. The applied methodology demonstrated strong capacity to differentiate levels of impact and capture patterns characteristic of Andean landscapes, where topography, vegetation type, and fuel continuity modulate fire intensity. These findings validate the use of dNBRc as a robust index adaptable to local ecological conditions and reinforce its utility for fire monitoring and management.

Temporal analysis of NDVI revealed significant vegetation degradation during the fires, followed by contrasting recovery trajectories among sites. While localities such as Pucará and San Felipe reached post-fire NDVI values exceeding pre-fire conditions, others such as Querocotillo, Miracosta, and San Juan exhibited limited recovery, indicating strong dependence on edaphic, climatic, and severity-related factors. These results underscore the

need to incorporate complementary ecological and climatic information in future studies, as well as to expand field validation efforts. Overall, the integration of satellite data and remote sensing methodologies applied in this study proves to be an effective tool for mapping fire severity and assessing vegetation resilience, providing key information for restoration planning, territorial management, and adaptive fire management in high Andean regions.

Acknowledgements
The authors acknowledge and appreciate the support of the Universidad Nacional de Jaen for providing logistical support for the development of the research.

Authors' contributions
Jefferson A. Cubas-Sánchez: Writing – original draft, Validation, Resources, Methodology, Investigation, Formal analysis, Data curation, Conceptualization. Candy L. Ocaña-Zúñiga : Writing – review & editing, Writing – original draft, Visualization, Supervision, Resources, Project administration, Methodology, Investigation, Funding acquisition, Data curation, Conceptualization. Heins Gonzales-Perez : Writing – original draft, Visualization, Software, Methodology, Investigation, Data curation, Conceptualization. Mario Ruiz-Ramos : Writing – review & editing, Writing – original draft, Validation, Software, Methodology, Investigation, Conceptualization. Almites Santos-Moreno : Writing – review & editing, Writing – original draft, Visualization, Validation, Software, Resources, Methodology, Investigation, Data curation, Conceptualization. Elgar Barboza : Writing – review & editing, Writing – original draft, Visualization, Validation, Software, Methodology, Investigation, Formal analysis, Data curation, Conceptualization. Alex J. Vergara : Writing – review & editing, Writing – original draft, Visualization, Validation, Supervision, Methodology, Investigation.

Funding
This research has been funded by the National University of Jaen within the framework of the Research, Innovation and Technological Development Projects Competition—PROINTEC 2020, Grant No. 001–2021-UNJ/PCO.

Data availability
The datasets used and/or analyzed during the current study are available from the corresponding author on reasonable request.

Declarations

Ethics approval and consent to participate
Not applicable.

Consent for publication
Not applicable.

Competing interests
The authors declare no competing interests.

Author details
[1]Escuela Académica Profesional de Ingeniería Forestal y Ambiental, Universidad Nacional de Jaén (UNJ), Carretera Jaén San Ignacio, KM 21, Jaén 06801, Peru. [2]Centro Experimental Yanayacu, Dirección de Servicios Estratégicos Agrarios (DSEA), Instituto Nacional de Innovación Agraria (INIA), Carretera Jaén San Ignacio Km 23.7, Jaén 06801, Peru. [3]Instituto de Investigación en Ciencia de Datos, Universidad Nacional de Jaén (UNJ), Carretera Jaén San Ignacio, Km 21, Jaén 06801, Peru. [4]Escuela Académica Profesional de Ingeniería Forestal, Universidad Nacional de Cajamarca (UNC), Jr. Bolivar Nº 1342, Jaén 06801, Peru. [5]Instituto de Investigación para el Desarrollo Sustentable de Ceja de Selva (INDES-CES), Universidad Nacional Toribio Rodríguez de Mendoza de Amazonas, Chachapoyas 01001, Peru. [6]Instituto de Investigación, Innovación y Desarrollo Para El Sector Agrario y Agroindustrial (IIDAA), Facultad de Ingeniería y Ciencias Agrarias, Universidad Nacional Toribio Rodríguez de Mendoza de Amazonas, Calle Higos Urco 342—Ciudad Universitaria, Chachapoyas 01000, Peru.

Received: 30 June 2025 Accepted: 16 December 2025
Published online: 15 January 2026

References

Añamuro-Luque, H.H., C.J. Larico-Mamani, C.E. Ruiz-Vásquez, O.M. Monteza-Rosales, and J. Quiñonez-Choquecota. 2020. Análisis de incendios forestales en pajonales andinos utilizando sistemas de información geográfica y teledetección, Macari – Puno. *Revista El Ceprosimad* 8 (2): 30–37. https://doi.org/10.56636/CEPROSIMAD.V8I2.96.

Biogeosciences, F., and K. Alperen Coskuner. 2022. Assessing the performance of MODIS and VIIRS active fire products in the monitoring of wildfires: A case study in Turkey. *Iforest - Biogeosciences and Forestry* 15 (2): 85. https://doi.org/10.3832/IFOR3754-015.

Botella, M.M.A., and M.A. Fernández. 2017. Estudio de la severidad post-incendio en la Comunidad Valenciana comparando los índices dNBR, RdNBR y RBR a partir de imágenes landsat 8. *Revista De Teledeteccion* 49 Special Issue: 33–47. https://doi.org/10.4995/raet.2017.7095.

Briones-Herrera, C.I., D.J. Vega-Nieva, N.A. Monjarás-Vega, J. Briseño-Reyes, P.M. López-Serrano, J.J. Corral-Rivas, E. Alvarado-Celestino, S. Arellano-Pérez, J.G. álvarez-González, A.D. Ruiz-González, W.M. Jolly, and S.A. Parks. 2020. Near real-time automated early mapping of the perimeter of large forest fires from the aggregation of VIIRS and MODIS active fires in Mexico. *Remote Sensing* 12 (12): 1–19. https://doi.org/10.3390/RS12122061.

Briones-Herrera, C. I., Silva-Cardoza, A. I., Vega-Nieva, D. J., & Briseño Reyes, J. (2022). *Manual de usuario de las herramientas de mapeo de área quemada y severidad de incendios forestales a partir de imágenes Sentinel*. http://forestales.ujed.mx/incendios2/.

Capador, A.Y.E., A.G.P. González, and D.P.A. Suarez. 2021. Análisis de la cobertura vegetal en incendios forestales mediante índices espectrales: Caso de estudio Cerros Orientales (Bogotá, Colombia). *Avances: Investigación En Ingeniería* 18 (1): 1–17. https://doi.org/10.18041/1794-4953/avances.1.6931.

Caraveo, C. L. A. 2013. *Evaluación de la recuperación vegetal en áreas con distinta severidad de fuego usando teledetección: Caso de estudio, Municipio de Ocampo*. Coahuila: Universidad Autónoma de Ciudad Juárez.

Carmo, M., J. Ferreira, M. Mendes, Á. Silva, P. Silva, D. Alves, L. Reis, I. Novo, and D. Xavier Viegas. 2022. The climatology of extreme wildfires in Portugal, 1980–2018: Contributions to forecasting and preparedness. *International Journal of Climatology* 42 (5): 3123–3146. https://doi.org/10.1002/JOC.7411. (JOURNAL:JOURNAL:10970088A;WGROUP:STRING:PUBLICATION).

Centro Nacional de Estimación Prevención y Reducción del Riesgo de Desastres (CENEPRED). (2022). *Escenario de riesgo por incendios forestales de la región Cajamarca*. https://www.gob.pe/cenepred.

Chuvieco, E. (2001). Fundamentos de teledetection espacial. In S. A. EDICIONES RIALP (Ed.), *(Fundamentals of remote sensing from space* (Segunda ed).

Çolak, E., and F. Sunar. 2020. The importance of ground-truth and crowdsourcing data for the statistical and spatial analyses of the NASA FIRMS active fires in the Mediterranean Turkish forests. *Remote Sensing Applications: Society and Environment* 19: 100327. https://doi.org/10.1016/j.rsase.2020.100327.

Comisión Nacional Forestal (CONAFOR). (2010). *Incendios forestales: Guía práctica para comunicadores* (Vol. 3).

Corner, B.R., R.M. Narayanan, and S.E. Reichenbach. 2003. Noise estimation in remote sensing imagery using data masking. *International Journal of Remote Sensing* 24 (4): 689–702. https://doi.org/10.1080/01431160210164271.

Dentoni, M. del C., & Muñoz, M. M. (2012). *Informe técnico N°1: Sistemas de evaluación de peligro de incendios*. https://www.argentina.gob.ar/sites/default/files/ambiente-itn1_pnmf.pdf.

Delcourt, C.J.F., A. Combee, B. Izbicki, M.C. Mack, T. Maximov, R. Petrov, B.M. Rogers, R.C. Scholten, T.A. Shestakova, D. van Wees, and S. Veraverbeke. 2021. Evaluating the differenced normalized burn ratio for assessing fire severity using Sentinel-2 imagery in northeast Siberian larch forests. *Remote Sensing* 13 (12): 2311. https://doi.org/10.3390/RS13122311.

Díaz-Delgado, R., and X. Pons. 2001. Spatial patterns of forest fires in Catalonia (NE of Spain) along the period 1975–1995. *Forest Ecology and Management* 147 (1): 67–74. https://doi.org/10.1016/s0378-1127(00)00434-5.

Ding, Y., M. Wang, Y. Fu, L. Zhang, and X. Wang. 2023. A wildfire detection algorithm based on the dynamic brightness temperature threshold. *Forests* 14 (3): 477. https://doi.org/10.3390/F14030477.

Dirección General Parlamentaria. (2019). *Carpeta Georeferencial región Cajamarca Perú*. https://www.congreso.gob.pe/Docs/DGP/GestionInformacionEstadistica/files/i-06-cajamarca.pdf.

Eckmann, T.C., D.A. Roberts, and C.J. Still. 2008. Using multiple endmember spectral mixture analysis to retrieve subpixel fire properties from MODIS. *Remote Sensing of Environment* 112 (10): 3773–3783. https://doi.org/10.1016/J.RSE.2008.05.008.

Escuin, S., R. Navarro, and P. Fernández. 2008. Fire severity assessment by using NBR (normalized burn ratio) and NDVI (normalized difference vegetation index) derived from LANDSAT TM/ETM images. *International Journal of Remote Sensing* 29 (4): 1053–1073. https://doi.org/10.1080/01431160701281072.

Estes, B.L., E.E. Knapp, C.N. Skinner, J.D. Miller, and H.K. Preisler. 2017. Factors influencing fire severity under moderate burning conditions in the Klamath Mountains, northern California, USA. *Ecosphere* 8 (5): e01794. https://doi.org/10.1002/ECS2.1794.

Fernández-García, V., Beltrán, M. D., Pinto, P. R., Fernández-Guisuraga, J. M., & Calvo, L. (2019). Uso de técnicas de teledetección para determinar la relación entre la historia de incendios y la severidad del fuego. *Teledetección. Hacia Una Visión Global Del Cambio Climático., August 2021*, 135–138.

Filicetti, A.T., R.A. Lapointe, and S.E. Nielsen. 2018. Effects of fire severity and woody debris on tree regeneration for exploratory well pads in jack pine (*Pinus banksiana*) forests. *Forests* 12 (10): 1330. https://doi.org/10.3390/F12101330.

Flores, R. A. G., G. J. G. Flores, E. D. R. González, R. A. Gallegos, V. P. Zarazúa, and M. S. Mena. 2021. Comparative analysis of spectral indices to locate and size levels of severity of forest fires. *Investigaciones Geográficas* 106:1–21. https://doi.org/10.14350/rig.60396.

Forkel, M., N. Carvalhais, J. Verbesselt, M.D. Mahecha, C.S.R. Neigh, and M. Reichstein. 2013. Trend change detection in NDVI time series: Effects of inter-annual variability and methodology. *Remote Sensing* 5 (5): 2113–2144. https://doi.org/10.3390/RS5052113.

Fraser, R.H., Z. Li, and J. Cihlar. 2000. Hotspot and NDVI differencing synergy (HANDS): A new technique for burned area mapping over boreal forest. *Remote Sensing of Environment* 74 (3): 362–376. https://doi.org/10.1016/S0034-4257(00)00078-X.

García-Llamas, P., S. Suárez-Seoane, A. Fernández-Manso, C. Quintano, and L. Calvo. 2020. Evaluation of fire severity in fire prone-ecosystems of Spain under two different environmental conditions. *Journal of Environmental Management* 271: 110706. https://doi.org/10.1016/j.jenvman.2020.110706.

Giglio, L., W. Schroeder, and C.O. Justice. 2016. The collection 6 MODIS active fire detection algorithm and fire products. *Remote Sensing of Environment* 178: 31–41. https://doi.org/10.1016/J.RSE.2016.02.054.

Gómez-Sánchez, E., J. de las Heras, M.E. Lucas-Borja, and D. Moya. 2017. Ajuste de metodologías para evaluar severidad de quemado en zonas semiáridas (SE peninsular): Incendio donceles 2012. *Revista de Teledetección* 49: 103–113. https://doi.org/10.4995/raet.2017.7121.

Gonçalves, J., E. de Castro, F. Loureiro, and P. Pereira. 2024. Assessment of forest fires impacts on geoheritage: A study in the Estrela UNESCO Global Geopark, Portugal. *International Journal of Geoheritage and Parks* 12 (4): 580–605. https://doi.org/10.1016/J.IJGEOP.2024.11.005.

Gonzáles, H., C.L. Ocaña, J.A. Cubas, D.J. Vega-Nieva, M. Ruíz, A. Santos, and E. Barboza. 2024. Impact of forest fire severity on soil physical and chemical properties in pine and scrub forests in high Andean zones of Peru. *Trees, Forests and People* 18: 100659. https://doi.org/10.1016/J.TFP.2024.100659.

González-Gutiérrez, I., J.F. Mas-Caussel, L.M. Morales-Manilla, and K.A. Oceguera-Salazar. 2020. Fiabilidad temática de puntos de calor e incendios forestales en Michoacán, México. *Revista Chapingo. Serie Ciencias Forestales y del Ambiente* 26 (1): 17–35. https://doi.org/10.5154/R.RCHSCFA.2019.01.011.

Güney, C.O., A. Mert, and S. Gülsoy. 2023. Assessing fire severity in Turkey's forest ecosystems using spectral indices from satellite images. *Journal of Forestry Research* 34 (6): 1747–1761. https://doi.org/10.1007/S11676-023-01620-7.

Guo, R., J. Yan, H. Zheng, and B. Wu. 2024a. Assessment of the analytic burned area index for forest fire severity detection using Sentinel and Landsat data. *Fire* 7 (1): 19. https://doi.org/10.3390/FIRE7010019.

Guo, Y., J. Wang, Y. Ge, and C. Zhou. 2024b. Global expansion of wildland-urban interface intensifies human exposure to wildfire risk in the 21st century. *Science Advances* 10 (45): 9587. https://doi.org/10.1126/SCIADV.ADO9587.(JOURNAL:JOURNAL:SCIADV;WEBSITE:WEBSITE:AAAS-SITE;REQUESTEDJOURNAL:JOURNAL:SCIADV;ISSUE:ISSUE:DOI).

Haney, A., M. Bowles, S. Apfelbaum, E. Lain, and T. Post. 2008. Gradient analysis of an eastern sand savanna's woody vegetation, and its long-term responses to restored fire processes. *Forest Ecology and Management* 256 (8): 1560–1571. https://doi.org/10.1016/J.FORECO.2008.07.004.

Hawbaker, T.J., V.C. Radeloff, A.D. Syphard, Z. Zhu, and S.I. Stewart. 2008. Detection rates of the MODIS active fire product in the United States. *Remote Sensing of Environment* 112 (5): 2656–2664. https://doi.org/10.1016/J.RSE.2007.12.008.

Ibarra-Bonilla, J.S., A. Pinedo-Alvarez, J.A. Prieto-Amparán, P. Siller-Clavel, E. Santellano-Estrada, A. Álvarez-Holguín, and F. Villarreal-Guerrero. 2024. Post-fire vegetation dynamics of a temperate mixed forest: An assessment based on the variability of Landsat spectral indices. *Trees, Forests and People* 17: 100648. https://doi.org/10.1016/J.TFP.2024.100648.

Instituto Nacional de Estadística e Informática (INEI). (2018). *Perú: Crecimiento y distribuciòn de la población, 2017*. https://www.inei.gob.pe/media/MenuRecursivo/publicaciones_digitales/Est/Lib1530/libro.pdf

Jaafari, A., E.K. Zenner, and B.T. Pham. 2018. Wildfire spatial pattern analysis in the Zagros Mountains, Iran: A comparative study of decision tree based classifiers. *Ecological Informatics* 43: 200–211. https://doi.org/10.1016/j.ecoinf.2017.12.006.

Justice, C.O., L. Giglio, S. Korontzi, J. Owens, J.T. Morisette, D. Roy, J. Descloitres, S. Alleaume, F. Petitcolin, and Y. Kaufman. 2002. The MODIS fire products. *Remote Sensing of Environment* 83 (1–2): 244–262. https://doi.org/10.1016/s0034-4257(02)00076-7.

Kala, C.P. 2023. Environmental and socioeconomic impacts of forest fires: A call for multilateral cooperation and management interventions. *Natural Hazards Research* 3 (2): 286–294. https://doi.org/10.1016/j.nhres.2023.04.003.

Key, C. H., & Benson, N. C. (2006). Landscape assessment (LA) sampling and analysis methods. *USDA Forest Service - General Technical Report RMRS-GTR , 164 RMRS-GTR*.

Kolanek, A., M. Szymanowski, and A. Raczyk. 2021. Human activity affects forest fires: The impact of anthropogenic factors on the density of forest fires in Poland. *Forests* 12 (6): 728. https://doi.org/10.3390/f12060728.

Kumar, S., and A. Kumar. 2022. Hotspot and trend analysis of forest fires and its relation to climatic factors in the western Himalayas. *Natural Hazards* 114 (3): 3529–3544. https://doi.org/10.1007/S11069-022-05530-5.

Kurbanov, E., O. Vorobev, S. Lezhnin, J. Sha, J. Wang, X. Li, J. Cole, D. Dergunov, and Y. Wang. 2022. Remote sensing of forest burnt area, burn severity, and post-fire recovery: A review. *Remote Sensing* 14 (19): 4714. https://doi.org/10.3390/RS14194714/S1.

Li, Z., A. Erb, Q. Sun, Y. Liu, Y. Shuai, Z. Wang, P. Boucher, and C. Schaaf. 2018. Preliminary assessment of 20-m surface albedo retrievals from sentinel-2A surface reflectance and MODIS/VIIRS surface anisotropy measures. *Remote Sensing of Environment* 217:352–365. https://doi.org/10.1016/J.RSE.2018.08.025.

Liu, N., J. Lei, W. Gao, H. Chen, and X. Xie. 2021. Combustion dynamics of large-scale wildfires. *Proceedings of the Combustion Institute* 38 (1): 157–198. https://doi.org/10.1016/j.proci.2020.11.006.

Lopes, V., LCdos Santos, and J. M. Trillo-Santamaría. 2025. The influence of forest fires on ecological, economic, and social trends in landscape dynamics in Portugal. *Land* 14 (6): 1273. https://doi.org/10.3390/LAND14061273/S1.

Lutes, D.C., R.E. Keane, J.F. Caratti, C.H. Key, N.C. Benson, S. Sutherland, and L.J. Gangi. 2006. FIREMON: Fire effects monitoring and inventory system. *Gen. Tech. Rep. RMRS-GTR-164* 1: 164. https://doi.org/10.2737/RMRS-GTR-164.

Mabaso, S., E. Seyama, S. Mamba, S. Ginindza, N. Mthupha, S. Kunene, M. Masuku, N. Msibi, L. Lushaba, F. Zwane, N. Nxumalo, W. Dlamini, M. Dlamini, P. Sihlongonyane, N. Hleta, M. Mabuza, L. Thwala, M. Mpapane, S. Mabaso, and M. Mpapane. 2022. Understanding the causes, socio-economic and environmental impacts of 2019 veld fires in the Kingdom of Eswatini. *Open Journal of Social Sciences* 10 (9): 202–225. https://doi.org/10.4236/JSS.2022.109014.

Mallikarjun, J., A. Gorbushina, Y. Kuzyakov, M. Koester, R. Castro, A. Yudina, K. Abdallah, F.J. Matus, and M.A. Dippold. 2025. Post-fire recovery of temperate and Mediterranean ecosystems: An interplay between fire severity, soil nutrients, and vegetation from early-stage to decadal-scale dynamics. *CATENA* 260: 109431. https://doi.org/10.1016/J.CATENA.2025.109431.

Marques, J.F., M.B. Alves, C.F. Silveira, A. Amaral e Silva, T.A. Silva, V.J. dos Santos, and M.L. Calijuri. 2021. Fires dynamics in the Pantanal: Impacts of

anthropogenic activities and climate change. *Journal of Environmental Management* 299: 113586. https://doi.org/10.1016/J.JENVMAN.2021.113586.

McLauchlan, K.K., P.E. Higuera, J. Miesel, B.M. Rogers, J. Schweitzer, J.K. Shuman, A.J. Tepley, J.M. Varner, T.T. Veblen, S.A. Adalsteinsson, J.K. Balch, P. Baker, E. Batllori, E. Bigio, P. Brando, M. Cattau, M.L. Chipman, J. Coen, R. Crandall, and A.C. Watts. 2020. Fire as a fundamental ecological process: Research advances and frontiers. *Journal of Ecology* 108 (5): 2047–2069. https://doi.org/10.1111/1365-2745.13403.

Meng, R., J. Wu, F. Zhao, B.D. Cook, R.P. Hanavan, and S.P. Serbin. 2018. Measuring short-term post-fire forest recovery across a burn severity gradient in a mixed pine-oak forest using multi-sensor remote sensing techniques. *Remote Sensing of Environment* 210: 282–296. https://doi.org/10.1016/j.rse.2018.03.019.

Mohajane, M., R. Costache, F. Karimi, Q. Bao. Pham, A. Essahlaoui, H. Nguyen, G. Laneve, and F. Oudija. 2021. Application of remote sensing and machine learning algorithms for forest fire mapping in a Mediterranean area. *Ecological Indicators* 129: 107869. https://doi.org/10.1016/j.ecolind.2021.107869.

Morante-Carballo, F., Lady Bravo-Montero, P. Carrión-Mero, A. Velastegui-Montoya, and E. Berrezueta. 2022. Forest fire assessment using remote sensing to support the development of an action plan proposal in Ecuador. *Remote Sensing* 14 (8): 1783. https://doi.org/10.3390/rs14081783.

Morfin-Ríos, J. E., Jardel P., E. J., Alvarado C., E., & Michel-Fuentes, J. M. (2012). Caracterización y cuantificación de combustibles forestales. In *Comisión Nacional Forestal-Universidad de Guadalajara. Guadalajara, Jalisco, México*.

Morresi, D., A. Vitali, C. Urbinati, and M. Garbarino. 2019. Forest spectral recovery and regeneration dynamics in stand-replacing wildfires of central Apennines derived from Landsat time series. *Remote Sensing*. https://doi.org/10.3390/rs11030308.

Naveh, Z. 1990. Fire in the Mediterranean - A landscape ecological perspective. *Fire in Ecosystems Dynamics* 3: 1–20.

Nemani, R. R., C. D. Keeling, H. Hashimoto, W. M. Jolly, S. C. Piper, C. J. Tucker, R. B. Myneni, and S. W. Running. 2003. Climate-driven increases in global terrestrial net primary production from 1982 to 1999. *Science* 300 (5625): 1560–1563. https://doi.org/10.1126/SCIENCE.1082750. (WEBSITE:WEBSITE:AAAS-SITE;JOURNAL:JOURNAL:SCIENCE;WGROUP:STRING:PUBLICATION).

Ouattara, B., M. Thiel, G. Forkuor, F. Mouillot, P. Laris, E.J. Tondoh, and B. Sponholz. 2025. Fire impacts, vegetation recovery, and environmental drivers in West African savannas (2014–2023): A high-resolution remote sensing assessment. *International Journal of Applied Earth Observation and Geoinformation* 143: 104783. https://doi.org/10.1016/J.JAG.2025.104783.

Parks, S.A., L.M. Holsinger, M.H. Panunto, W.M. Jolly, S.Z. Dobrowski, and G.K. Dillon. 2018. High-severity fire: Evaluating its key drivers and mapping its probability across western US forests. *Environmental Research Letters* 13 (4): 044037. https://doi.org/10.1088/1748-9326/aab791.

Pérez-Cabello, F., R. Montorio, and D.B. Alves. 2021. Remote sensing techniques to assess post-fire vegetation recovery. *Current Opinion in Environmental Science & Health*. https://doi.org/10.1016/j.coesh.2021.100251.

Pettorelli, N., Ryan, S., Mueller, T., Bunnefeld, N., Jedrzejewska, B., Lima, M., Kausrud, K. 2011. The Normalized Difference Vegetation Index (NDVI): Unforeseen successes in animal ecology. *In Climate Research* 46 (1): 15–27. https://doi.org/10.3354/cr00936; https://www.jstor.org/stable/24872307.

Piao, Y., D. Lee, S. Park, H.G. Kim, and Y. Jin. 2022. Forest fire susceptibility assessment using Google Earth Engine in Gangwon-do, Republic of Korea. *Geomatics, Natural Hazards and Risk* 13 (1): 432–450. https://doi.org/10.1080/19475705.2022.2030808.

Plank, S., E.M. Fuchs, and C. Frey. 2017. A fully automatic instantaneous fire hotspot detection processor based on AVHRR imagery—a TIMELINE thematic processor. *Remote Sensing* 9 (1): 30. https://doi.org/10.3390/RS9010030.

Qian, Y., G. Yan, S. Duan, and X. Kong. 2009. A contextual fire detection algorithm for simulated HJ-1B imagery. *Sensors* 9 (2): 961–979. https://doi.org/10.3390/S90200961.

Rouse, J. W., Jr., Haas, R. H., Schell, J. A., Deering, D. W. 1973. Monitoring vegetation systems in the Great Plains with ERTS (NASA Goddard Space Flight Center 3d ERTS-1 Symposium, Vol. 1, Sect. A, Paper A20). NASA Technical Reports Server.https://ntrs.nasa.gov/api/citations/19740022614/downloads/19740022614.pdf.

Ryu, J.H., S.. . Il.. Na, and J. Cho. 2020. Inter-comparison of normalized difference vegetation index measured from different footprint sizes in cropland. *Remote Sensing* 12 (18): 2980.

Santana, N.C. 2018. Fire recurrence and normalized difference vegetation index (NDVI) dynamics in Brazilian savanna. *Fire* 2 (1): 1.

Shvetsov, E.G., E.A. Kukavskaya, L.V. Buryak, and K. Barrett. 2019. Assessment of post-fire vegetation recovery in Southern Siberia using remote sensing observations. *Environmental Research Letters* 14 (5): 055001. https://doi.org/10.1088/1748-9326/ab083d.

Sidhu, N., E. Pebesma, and G. Câmara. 2018. Using Google Earth Engine to detect land cover change: Singapore as a use case. *European Journal of Remote Sensing* 51 (1): 486–500. https://doi.org/10.1080/22797254.2018.1451782.

Silva-Cardoza, A. I., Vega-Nieva, D. J., Serrano, P. M. L., Rivas, J. J. C., Trejo, D. A. R., Peláez, E. J., & Balcázar, O. (2021). *Metodología para la evaluación de la severidad de incendios forestales en campo, en ecosistemas de bosque templado de México*.

Silva-Cardoza, A.I., D.J. Vega-Nieva, J. Briseño-Reyes, C.I. Briones-Herrera, P.M. López-Serrano, J.J. Corral-Rivas, S.A. Parks, and L.M. Holsinger. 2022. Evaluating a new relative phenological correction and the effect of Sentinel-based earth engine compositing approaches to map fire severity and burned area. *Remote Sensing* 14 (13): 3122.

Singh, S., H. Singh, V. Sharma, V. Shrivastava, P. Kumar, S. Kanga, N. Sahu, G. Meraj, M. Farooq, and S.K. Singh. 2022. Impact of forest fires on air quality in Wolgan Valley, New South Wales, Australia—a mapping and monitoring study using Google Earth Engine. *Forests* 13 (1): 4.

Sistema de Información Ambiental Regional (SIAR). (2019). *Monitoreo de las condiciones favorables para la ocurrencia de incendios en Cajamarca | SIAR Cajamarca | Sistema de Información Ambiental Regional de Cajamarca*. https://siar.regioncajamarca.gob.pe/novedades/monitoreo-las-condiciones-favorables-ocurrencia-incendios-cajamarca.

Sistema Nacional de Evaluación Acreditación y Certificación de la Calidad Educativa (Sineace). (2020). *Caracterización de la región Cajamarca*. https://repositorio.sineace.gob.pe/repositorio/bitstream/handle/20.500.12982/6228/Caracterizaci%C3%B3n%20Regional%20Cajamarca.pdf?sequence=1&isAllowed=y.

Smith, D., D. Anderson, A. D. Degryse, C. Bol, A. Criado, A. Ferrara, N. H. Franco, I. Gyertyan, J. M. Orellana, G. Ostergaard, O. Varga, and H. M. Voipio. 2018. Classification and reporting of severity experienced by animals used in scientific procedures: FELASA/ECLAM/ESLAV Working Group report. *Laboratory Animals* 52 (1 Suppl): 5. https://doi.org/10.1177/0023677217744587.

Spadoni, G.L., A. Cavalli, L. Congedo, and M. Munafò. 2020. Analysis of normalized difference vegetation index (NDVI) multi-temporal series for the production of forest cartography. *Remote Sensing Applications: Society and Environment* 20: 100419. https://doi.org/10.1016/j.rsase.2020.100419.

Stevens-Rumann, C.S., A.T. Hudak, P. Morgan, A. Arnold, and E.K. Strand. 2020. Fuel dynamics following wildfire in US Northern Rockies Forests. *Frontiers in Forests and Global Change* 3: 527342. https://doi.org/10.3389/FFGC.2020.00051.

Storey, E.A., D.A. Stow, and J.F. O'Leary. 2016. Assessing postfire recovery of chamise chaparral using multi-temporal spectral vegetation index trajectories derived from Landsat imagery. *Remote Sensing of Environment* 183: 53–64. https://doi.org/10.1016/j.rse.2016.05.018.

Sudhakar, S., V. Vijayakumar, C. Sathiya Kumar, V. Priya, L. Ravi, and V. Subramaniyaswamy. 2020. Unmanned aerial vehicle (UAV) based forest fire detection and monitoring for reducing false alarms in forest-fires. *Computer Communications* 149: 1–16. https://doi.org/10.1016/j.comcom.2019.10.007.

Suresh Babu, K.V., A. Roy, and P.R. Prasad. 2016. Forest fire risk modeling in Uttarakhand Himalaya using TERRA satellite datasets. *European Journal of Remote Sensing* 49: 381–395. https://doi.org/10.5721/EuJRS20164921.

Tangney, R., R.G. Miller, J.B. Fontaine, W.P. Veber, K.X. Ruthrof, and B.P. Miller. 2022. Vegetation structure and fuel dynamics in fire-prone, Mediterranean-type Banksia woodlands. *Forest Ecology and Management* 505: 119891. https://doi.org/10.1016/J.FORECO.2021.119891.

Tonbul, H., T. Kavzoglu, and S. Kaya. 2016. Assessment of fire severity and post-fire regeneration based on topographical features using multi-temporal Landsat imagery: A case study in Mersin, Turkey. *International Archives of the Photogrammetry, Remote Sensing and Spatial Information Sciences - ISPRS Archives* 41:763–769. https://doi.org/10.5194/isprsarchives-XLI-B8-763-2016.

Vales, J.J., I. Pino, L. Granado, R. Prieto, E. Méndez, M. Rodríguez, F. de Giménez Azcárate, E. Ortega, and J.M. Moreira. 2020. Cartografía de la afección y recuperación vegetal del incendio de Las Peñuelas en Moguer (Huelva) con imágenes satelitales. Año 2017. *Revista De Teledetección* 57: 79. https://doi.org/10.4995/raet.2020.13082.

Veraverbeke, S., S. Hook, and G. Hulley. 2012. An alternative spectral index for rapid fire severity assessments. *Remote Sensing of Environment* 123:72–80. https://doi.org/10.1016/J.RSE.2012.02.025.

Vetrita, Y., Cochrane, M. A., Suwarsono, Priyatna, M., Sukowati, K. A. D., & Khomarudin, M. R. (2021). Evaluating accuracy of four MODIS-derived burned area products for tropical peatland and non-peatland fires. *Environmental Research Letters*, *16*(3), 035015. https://doi.org/10.1088/1748-9326/ABD3D1.

Vilchis-Francés, A. Y., C. Díaz-Delgado, D. Magaña-Lona, K. M. Bâ, and M. Á. Gómez-Albores. 2015. Modelado espacial para peligro de incendios forestales con predicción diaria en la cuenca del río Balsas. *Agrociencia* 49 (7): 803–20.

Vlassova, L., Rosero, T. P., & Montorio, L. R. (2016). Variabilidad espacio-temporal de la temperatura de superficie en ecosistemas de dehesa estimada mediante imágenes Landsat TM: el papel del arbolado. *Geographicalia*, 69–86. https://doi.org/10.26754/ojs_geoph/geoph.2016681582

Vo, V.D., and A.M. Kinoshita. 2020. Remote sensing of vegetation conditions after post-fire mulch treatments. *Journal of Environmental Management* 260: 109993. https://doi.org/10.1016/j.jenvman.2019.109993.

White, J.D., K.C. Ryan, C.C. Key, and S.W. Running. 1996. Remote sensing of forest fire severity and vegetation recovery. *International Journal of Wildland Fire* 6 (3): 125–136. https://doi.org/10.1071/WF9960125.

Xie, P., Z.G. Yang, F. Liu, and X. Wu. 2025. Drivers of short-term recovery in vegetation greenness and canopy height in burned areas of Southwest China. *Environmental and Sustainability Indicators* 28: 100950. https://doi.org/10.1016/J.INDIC.2025.100950.

Yang, Z., M. Zhang, L. Wang, X. Su, and W. Qin. 2023. Diurnal time representation of MODIS, VIIRS, MISR, and AHI over Asia and Oceania. *Remote Sensing of Environment* 299: 113878. https://doi.org/10.1016/J.RSE.2023.113878.

Zahabnazouri, S., P. Belmont, S. David, P.E. Wigand, M. Elia, and D. Capolongo. 2025. Detecting burn severity and vegetation recovery after fire using dNBR and dNDVI indices: Insight from the Bosco Difesa Grande, Gravina in Southern Italy. *Sensors* 25 (10): 3097. https://doi.org/10.3390/S25103097.

Zahura, F.T., G. Bisht, Z. Li, S. McKnight, and X. Chen. 2024. Impact of topography and climate on post-fire vegetation recovery across different burn severity and land cover types through random forest. *Ecological Informatics* 82: 102757. https://doi.org/10.1016/J.ECOINF.2024.102757.

Zewdie, W., E. Csaplovics, and L. Inostroza. 2017. Monitoring ecosystem dynamics in northwestern Ethiopia using NDVI and climate variables to assess long term trends in dryland vegetation variability. *Applied Geography* 79:167–178. https://doi.org/10.1016/J.APGEOG.2016.12.019.

Zhang, Q.X., G.H. Lin, Y.M. Zhang, G. Xu, and J.J. Wang. 2018. Wildland forest fire smoke detection based on faster R-CNN using synthetic smoke images. *Procedia Engineering* 211: 441–446. https://doi.org/10.1016/j.proeng.2017.12.034.

Publisher's Note